Molecular Biology of the Cell
Vol. 14, 3169–3179, August 2003

TINA Interacts with the NIMA Kinase in *Aspergillus nidulans* and Negatively Regulates Astral Microtubules during Metaphase Arrest[V]

Aysha H. Osmani, Jonathan Davies, C. Elizabeth Oakley, Berl R. Oakley, and Stephen A. Osmani*

Department of Molecular Genetics, The Ohio State University, Columbus, Ohio 43210

Submitted November 8, 2002; Revised March 13, 2003; Accepted March 28, 2003
Monitoring Editor: Mark Solomon

The *tinA* gene of *Aspergillus nidulans* encodes a protein that interacts with the NIMA mitotic protein kinase in a cell cycle-specific manner. Highly similar proteins are encoded in *Neurospora crassa* and *Aspergillus fumigatus*. TINA and NIMA preferentially interact in interphase and larger forms of TINA are generated during mitosis. Localization studies indicate that TINA is specifically localized to the spindle pole bodies only during mitosis in a microtubule-dependent manner. Deletion of *tinA* alone is not lethal but displays synthetic lethality in combination with the anaphase-promoting complex/cyclosome mutation *bimE7*. At the *bimE7* metaphase arrest point, lack of TINA enhanced the nucleation of bundles of cytoplasmic microtubules from the spindle pole bodies. These microtubules interacted to form spindles joined in series via astral microtubules as revealed by live cell imaging. Because TINA is modified and localizes to the spindle pole bodies at mitosis, and lack of TINA causes enhanced production of cytoplasmic microtubules at metaphase arrest, we suggest TINA is involved in negative regulation of the astral microtubule organizing capacity of the spindle pole bodies during metaphase.

INTRODUCTION

Mitosis is regulated by cell cycle-specific phosphorylation and regulated proteolysis of regulatory proteins mediated by activation and inactivation of cyclin-dependent kinases (CDKs) (O'Farrell, 2001) in all eukaryotes, including *Aspergillus nidulans* (Osmani and Ye, 1996). In *A. nidulans*, mitosis is also regulated by a second kinase, NIMA (***n***ever ***i***n ***m***itosis **A**), which when inactivated arrests cell in G_2 even though the CDK1 complex is active (Osmani *et al*., 1991a). Without activation of NIMA, active CDK1 is unable to accumulate in the nucleus but does so after mutation of the nuclear pore complex protein $SONA^{rae1/gle2}$ (Wu *et al*., 1998). NIMA may therefore interact with the nuclear pore complex to help mediate localization of CDK1 at mitosis.

NIMA is regulated at multiple levels, including mRNA abundance (Osmani *et al*., 1987), phosphorylation (Ye *et al*., 1995; Pu *et al*., 1995), and proteolysis (Pu and Osmani, 1995;Ye *et al*., 1998). NIMA has also been shown to have a dynamic localization during mitosis being sequentially located to DNA, the mitotic spindle, and the spindle pole body (SPB) (De Souza *et al*., 2000).

Expression of NIMA promotes chromatin condensation (O'Connell *et al*., 1994) and transient formation of mitotic spindle-like structures (Osmani *et al*., 1988b). Stable versions of NIMA prevent normal exit from mitosis (Pu and Osmani, 1995). The mitotic promoting activity of NIMA crosses species barriers from yeast to humans (Lu and Hunter, 1995a), indicating conserved NIMA substrates are involved in mitotic regulation.

NIMA-related kinases have been isolated from *Neurospora crassa* (Pu *et al*., 1995) and *Schizosaccharomyces pombe* (Krien *et al*., 1998), and the *S. pombe* NIMA-like kinase Fin1p is involved in mitotic regulation (Grallert and Hagan, 2002; Krien *et al*., 2002). ***N***IMA-***r***elated ***k***inases (NEKs) have also been identified in higher eukaryotes (Letwin *et al*., 1992; Schultz and Nigg, 1993; Lu and Hunter, 1995b; Chen *et al*., 1999; Tanaka and Nigg, 1999; Uto and Sagata, 2000; Kandli *et al*., 2000; Holland *et al*., 2002; Roig *et al*., 2002), some of which have been implicated in cell cycle progression.

NEK2 is regulated through the cell cycle (Schultz *et al*., 1994; Fry *et al*., 1995) and has been localized to, and been shown to regulate, the centrosome (Fry *et al*., 1998b; Uto and Sagata, 2000) through interactions with the centrosomal protein C-nap1 (Fry *et al*., 1998a) and protein phosphatase type 1 (Helps *et al*., 2000). Additional roles for NEK2 during cell cycle progression are suggested by the localization of NEK2

Article published online ahead of print. Mol. Biol. Cell 10.1091/mbc.E02–11–0715. Article and publication date are available at www.molbiolcell.org/cgi/doi/10.1091/mbc.E02–11–0715.

[V] Online version of this article contains video material for some figures. Online version is available at www.molbiolcell.org.

* Corresponding author. E-mail address: osmani.2@osu.edu.

to meiotic (Rhee and Wolgemuth, 1997) and mitotic chromosomes (Ha *et al*., 2002). Recent studies have identified the Nercc1 kinase as a binding partner of Nek6, which is involved in chromosome alignment and segregation at mitosis and contains an RCC1-like domain (Roig *et al*., 2002).

Little is known about how NIMA kinases help to bring about the dramatic changes in microtubule dynamics and chromosome architecture seen during mitosis, although NIMA has been proposed to act as a histone H3 kinase at mitosis (De Souza *et al*., 2000). Isolation of proteins that interact with NIMA-like kinases may help to understand their role in cell cycle progression. We report herein on the TINA protein that interacts with NIMA and displays characteristics of a protein involved in mitotic microtubule function.

MATERIALS AND METHODS

Aspergillus Genetics, Immunofluorescence, and Protein Analysis

Standard media and genetic methods were used for culture of *A. nidulans* and to generate appropriate strains (Pontecorvo, 1953). 4,6-Diamidino-2-phenylindole (DAPI) staining, protein extraction, immunoprecipitation, immunofluorescence, and *A. nidulans* transformation and analysis were as described previously (Osmani *et al*., 1987; Oakley and Osmani, 1993; Ye *et al*., 1995). TINA was hemagglutinin (HA)-tagged after cloning into the expression vector pAL5 (Doonan *et al*., 1991) by using a method based upon the Stratagene (La Jolla, CA) QuikChange mutagenesis kit (Wu *et al*., 1998). *tinA* was first amplified by polymerase chain reaction (PCR) from plasmid pAO13 by using primers AO95 (5′-ATAGGTACCATCATGGAGCAGCAAGGTGAT) and AO96 (5′-GTCGGATCCCTACTTCATGCCCAGTAACTC), which introduced 5′ *Kpn*I and 3′ *Bam*HI sites for cloning into pAL5. Two copies of the HA tag were introduced at the 3′ end of *tinA* by using primers AO105 (5′-TACCCATACGATGTTCCTGACTATGCGGGCTATCCCTATGACGTCGCGGACTATGCAGGATAGGGA-TCCTCTAGAG-TCGAGCTTGCTGG) and AO106 (5′-TCCTGCATAGTCCGGGACGTCATAGGGATAGCCCGCATAGTCAGGAACATCGTATGGGTACTTCATGCCCAGTAACTCCCCCAG) as described previously (Wu *et al*., 1998) to generate plasmid pAO58. pAO58 was transformed into strain GR5 and inducible expression confirmed via Western blotting by using 12CA5 α-HA antibodies. A transformant was selected for further analysis named SO178. For coimmunoprecipitation experiments a homozygous *nimT23* diploid was generated (D31) from haploid SO223 that contained *alcA*::HA-*tinA* (derived from crosses of strain SO178) and haploid SO233 derived from strain 5C (Osmani *et al*., 1988b) containing *alcA*::*nimA*. Diploid D31 was grown in minimal media supplemented with 5 g/l yeast extract and 20 g/l lactose and 40 mM threonine to early log phase at 22°C. After shifting to the restrictive temperature of 42°C for 3 h to arrest cells in G_2, cells were placed at 30°C to allow synchronous entry into mitosis. For coimmunoprecipitation, 5 mg of protein was treated with 20 μl of affinity-purified α-NIMA antibodies raised in sheep by using the ANYRED peptide as immunogen (Ye *et al*., 1996) or 25 μl of 12CA5. Immunoprecipitates were collected using biotinylated donkey anti-rabbit antibodies or biotinylated goat anti-mouse antibodies and Streptavidin MagneSphere Paramagnetic particles (Promega, Madison, WI) followed by extensive washing in HK buffer (Osmani et al., 1991b). After Western blot transfer, precipitated proteins were visualized using E14 (1/600) or 12CA5 (1/600) antibodies. Protein extracts for straight Western blotting were prepared by boiling 5 mg of freeze-dried mycelia ground to a fine powder in 200 μl of 2× SDS sample buffer containing 6 M urea.

cDNA Library Construction

Strain R153 was grown in YG media to log phase and RNA was isolated from mycelia by using the Ultraspec-II RNA isolation system (Biotecx, Houston, TX). PolyA^+ mRNA was purified from total RNA by using the Poly-A Tract mRNA isolation system (Promega). cDNA synthesis was completed using the HybriZAP two-hybrid cDNA Gigapack cloning kit (Stratagene). Size-fractionated cDNA (>500 base pairs) was directionally cloned into the HybriZAP vector to generate a library of 1.9×10^6 primary clones. Portions of the primary library and amplified library were excised to generate the pAD-GAL4 phagemid library. Analysis of 32 random clones indicated an average insert size of 0.9 kb with all clones having an insert. The library was screened using the *nimA* constructs described below and standard procedures as outlined in the HybriZAP two-hybrid cDNA gigapack cloning kit (Stratagene).

Construction of nimA Baits and Rapid Amplification of cDNA Ends Analysis

Full-length nimA cDNA was cloned as a *Nco*I-*Hinc*II fragment into pAS2-1 (BD Biosciences Clontech, Palo Alto, CA) to generate plasmid pAO7. Two kinase negative forms of *nimA* (K40M and T199A) were generated using the QuikChange mutagenesis kit (Stratagene) to generate plasmids pAO8 and pAO10, respectively. A 3′-truncated *nimA* clone was generated as a *Nco*I-*Pst*I fragment cloned into pAS2-1 to generate pAO6 and a 5′- + 3′-truncated version as a *Eco*RI-*Pst*I fragment in vector pBD-Gal4 to generate pAO1. Rapid amplification of cDNA ends analysis was completed as described previously (Bussink and Osmani, 1998).

GFP Tagging and Antibody Production

The *tinA* open reading frame was amplified by PCR incorporating 5′ *Spe*I and 3′ *Not*I sites by using primers AO229 (5′-GGACTAGTACGTCCATCATGGAGCAGCAA) and AO230 (5′-CTGAGCGGCCGCCTTCATGCCCAGTAACTCCCC). The *Spe*I site was used to introduce a *Kpn*I site by using an adapter approach before cloning into a vector (pCDS15; Osmani and De Souza, unpublished data), driving expression from the *alcA* promoter a fusion of TINA to plant-adapted green fluorescent protein (GFP) (Fernandez-Abalos *et al*., 1998). To visualize microtubules, a plasmid containing GFP-tagged *tubA* under control of its own promoter (pLO76) was generated. Plasmid pLO76 was constructed as follows. A 500-base pair EcoR1-*Xma*I fragment carrying the *tubA* promoter was amplified by PCR from plasmid pDP485 (Doshi *et al*., 1991) by using primers TUBANCF (cagaattcatgcagcacgtgactatt) and TUBANCR (ccaaccgggcatcttgtctaggtgggt), and digested with EcoR1 and *Xma*I before ligation. An *Xma*I-*Xma*I fragment carrying a sequence encoding GFP 2-5 fused to *tubA* was amplified from pGFPtubA [online supplementary material to Han *et al*., 2001 (http://images.cellpress.com/supmat/cub/2001.htm#Volume_11_Issue_9)] by using primers GFPTUBAF (ccaacccgggagtaaaggagaagaactt) and TUBANCR2 (ccaacccggggcaaggccagcagattta). This fragment was digested with *Xma*I before ligation. The two fragments were ligated to plasmid pPL6 (see below), which had been digested with EcoR1 and *Xma*I. Appropriate restriction digests revealed that pLO76 carries the two PCR products in the desired orientation, giving a GFP-*tub*A fusion under the control of the endogenous *tubA* promoter.

Plasmid pLO76 was transformed into *A. nidulans* strain SO6 and the resulting transformants were screened for GFP fluorescence of microtubules. The wild-type *tubA* gene was evicted using 5-fluoroorotic acid (Dunne and Oakley, 1988), leaving the GFP-*tubA* allele in strain LO1016. The GFP-*tubA* was then introduced into other strains by genetic crosses.

Plasmid pPL6 was constructed as follows. The *pyrG* gene was obtained as a 1.4-kb fragment from an *Nde*I/*Xho*I double digest of pJR15 (Oakley *et al*., 1987). The *Xho*I site is 458 base pairs 5′ to the start codon and the *Nde*I site is 43 base pairs 3′ to the termination codon. This fragment was inserted into the blunted *Nde*I site of pUC19, leaving the polycloning site intact.

Time-lapse GFP-tubulin images were collected using an Eclipse TE300 inverted microscope (Nikon, Tokyo, Japan) fitted with an

Ultraview spinning-disk confocal system (PerkinElmer Life Sciences, Boston, MA) and a ORCA-ER digital camera (Hamamatsu, Bridgewater, NJ). For temperature-shift experiments, a delta T4 culture system was used in combination with an objective heater system (Bioptechs, Butler, PA). Peptide-specific antibodies were generated against the C-terminal 14 amino acids of TINA with a N-terminal cysteine added (CTLTSDELGELLGMK) for cross-linking to a KLH carrier. The peptide was synthesized, linked to KLH and used to immunize rabbits and antiserum affinity purified by Bethyl Laboratories (Montgomery, TX).

Aspergillus nidulans Strains

5C (*pyrG89 + alcA:nimA pyr4*$^{+}$; *fwA1*; *benA22*; *pabaA1*). D31 (diploid between SO223 and SO233). DBE4 (*bimE7:riboA2;pyrG89*). GR5 (*pyroA4*; *pyrG89*; *wA3*). LO1016 (GFP-*tubA; nimA5*; *wA2;*; *yA2*; *chaA1*; *pyrG89*; *cnxE16*; sC12; *choA1*) LO1029 (GFP-*tubA*; *pabaA1*; *choA1*; *pyrG89*; *fwA1*) LPW75 (*nimA5*; *choA1*; *pyrG89*; *fwA1*). SO6 (*nimA5*; *wA2;*; *yA2*; *chaA1*; *pyrG89*; *cnxE16*; sC12; *choA1*) SO182 (*nimT23*; *pyrG89*; *pabaA1*; *chaA1*). SO223 (*pyrG89 + alcA:nimA pyr4*$^{+}$; *nimT23*; *pabaA1*; *fwA1*). SO233 (*pyrG89 + alcA:tinA*-HA *pyr4*$^{+}$; *nimT23*; *pyroA4*; *wA3*). SO291 and SO292 (*pyrG89 + ΔtinA::pyrG+ZEO*; *pyroA4*; *wA3*). SO326 (*bimE7*; *ΔtinA::pyrG+ZEO; pyroA4; riboA2; wA3*). SO327 (*bimE7*; *ΔtinA::pyrG+ZEO; riboA2; wA3*). SO429 (*bimE7*; *ΔtinA::pyrG*; [*pyrG89*]; GFP-*tubA*; *wA3*; *pabaA1*). SO430 (*bimE7*; GFP-*tubA*; *wA3*; *choA1*).

Deletion of tinA by Using BAC Recombination

Two BAC clones (27M21 and 31G32) containing *tinA* were identified from an *A. nidulans* genomic BAC library made by Dr. Ralph Dean and obtained from Clemson University Genomics Institute (http://www.genome.clemson.edu/) by hybridization with *tinA* cDNA as a probe with standard techniques (Sambroook *et al*., 1989). These BACs were introduced into *Escherichia coli* stain DY380 (Lee *et al*., 2001) in which the recombination genes *exo*, *bet*, and *gam* are under the control of the temperature-sensitive λ cI-repressor (Yu *et al*., 2000; Swaminathan *et al*., 2001). A deletion cassette containing *Aspergillus fumigatus pyrG* and zeocin resistance (ZEO) was amplified from plasmid pCDA21 (Chaveroche *et al*., 2000) by using primers TINApyr (5′-GAGGACATCACCTCGGTTTTAAAACTACATTATCTCAGGCTGCTTGCAGG//GAATTCGCCTCAAACAATGC) and TINAzeo (5′-GGGTATATGACGGTTTGACGCTACTTCATGCCCAGTAACTCCCCCAGCTCA//GGAATTCTCAGTCCTGCTCC) with 50 base pairs of homology to the flanking regions of the *tinA* open reading frame. The BAC containing DY380 strains were induced for recombination at 42°C and electroporated with the deletion cassette as described previously (Swaminathan *et al*., 2001). Correct deletion of *tinA* in the BAC clones was confirmed by PCR by using primers AO180 (5′ CTTGGCCGTATAGATTCTGG) and AO190 (5′ ACATCGGTGCTGTATTCCTC). Either linear or uncut BAC DNA was used to transform strain GR5 by using standard protocols (Osmani *et al*., 1987). Transformants were tested for heterokaryons to determine whether *tinA* may be essential (Osmani *et al*., 1988a) by growth of transformant conidia on media with and without uridine and uracil. Conidia from all transformants tested grew on both media indicating *tinA* is not an essential gene or that it had not been successfully deleted in the tested transformants. Twenty transformants were therefore streaked to single colony three times before confirming clean deletion of *tinA* by using PCR, Southern blot analysis, and Western blotting. Equal loading and transfer of protein was confirmed by Ponceau Red staining of nitrocellulose filters during Western blotting.

```
TINA   DLQAASNYINNVLLARGLVKSGRPIDFANPENEEGGVATTMARIINLVNDLVLRRDREAE 65
       +L+ AS YINN LL+RGL++ G  IDFA P + +  +A TM RI+ +VNDL+LRRDR+AE
TIN-A NLRTASIYINNQLLSRGLLRDGDTIDFAYPGDNDDELAHTMGRIMGVVNDLILRRDRDAE 65

TINA   HRENLATTIRTLRAEESHKAVEMEKLQTKKSELSRSLALAEAQERALKTSMSSAEATIRG 125
        RE+L+ T+R+LRAE   ++ ++ +L  K ++ +R  ALAE +    +  + +AE T+
TIN-A TRESLSQTLRSLRAESLRQSTDIVRLSDKLTDSARKTALAEQETAHARAQLKAAEQTVAR 125

TINA   LKDQVQRMKTTVQQVRSQCANDIRKRDLELQKLKAHLAD--RQRG-------KRD-GLGV 175
       LK++  R K+ VQQ R+ CAN+IRKRD  ++ LK  +AD  R RG         RD G+G
TIN-A LKEEAARQKSLVQQTRNACANEIRKRDRMIEGLKKAVADAGRTRGTGHTRGASRDGGMGS 185

TINA   TTININPAASQSSRRYLSGGEG--------VHDPGYSLKQETNEFLTQLLQNLSDENDSL 227
           +     Q+   Y +   G             GY L+ ETN FL +L + LS+EN+ L
TIN-A GLGGVMSIVVQAGEEYNAEAGGKMGVPQGMTGSEGYDLRMETNGFLAELAKGLSEENEVL 245

TINA   ISLARNTVFTLKELQG-----------LSSTEEPAVDNG---YLQGSASTAQRSTYGGAA 273
       + L R TV  ++E+ G                ++   D G    ++G     +    G
TIN-A LGLVRRTVKRMQEMSGWDVVANVVVHQQQQQQQQQKDEGGDTNMEGGGELRKEEDEGEKH 305

TINA   VTSLPASCEELSGEMDQVLEHLRTLLTNPSFVPLEEVEVRDEEIKRLREGWEKMESRWRQ 333
          +P SCEEL  +++ VLEH+R +LTNPSFVP+EEV VR++EI RLR+GW KMESRW++
TIN-A ALVIPTSCEELQRDLENVLEHMRIILTNPSFVPIEEVVVREDEIHRLRDGWVKMESRWKE 365

TINA   AVTMMDGWHKRIAHGGGSVRAEELRMGLKLN 364
       AV ++DGW  R+   G +V  EEL+MGL+L+
TIN-A AVHLIDGWRNRMQVSGKAVNVEELKMGLRLS 396
```

Figure 1. Sequence comparison of TINA and TIN-A. Alignment of amino acids 6–364 of *A. nidulans* TINA with a conceptual protein (NCU04570.1, termed TIN-A herein) of *N. crassa* identified using TBLASTN to search the genome sequence data at the Neurospora Sequencing Project, Whitehead Institute/MIT Center for Genome Research (www-genome.wi.mit.edu) assembly version 3 for proteins with similarity to TINA.

RESULTS

tinA Encodes a Protein That Interacts with NIMA in the Yeast Two-Hybrid System

To isolate NIMA interactive proteins that may be involved in mitotic regulation, we generated a cDNA library from growing mycelium of *A. nidulans* and used it in a two-hybrid screen with kinase negative and kinase positive versions of NIMA. The genes defined by the clones isolated were termed *tinA* through to *tinF* for ***t***wo-hybrid ***i***nteractors of **N**IMA. Of the six *tin* genes isolated *tinA* interacted most strongly with all versions of *nimA*, both kinase negative and positive, with β-Gal activities ranging from 77.5 U for full-length active NIMA to 19.1 U for 3′-truncated NIMA. No interaction was detected using control p53 bait or with *tinA* alone.

Molecular Analysis of tinA

tinA encodes a novel protein of 553 amino acids with a predicted molecular mass of 62 kDa. Sequence data have been submitted to GenBank under accession number AY272054. TINA has no distinguishing features apart from three high scoring potential coiled-coil domains (our unpublished data). No significant protein matches were identified at the National Center for Biotechnology Information blast site (highest BLAST alignment score of 43, Expect value [E] of 0.01). However, the genome of *N. crassa* (Neurospora Sequencing Project; Whitehead Institute/MIT Center for Genome Research, Cambridge, MA; www-genome.wi.mit.edu) encodes a protein (contig 3.235, scaffold 15) with a BLAST alignment score of 228 and an E value of 2e-59 over a region of TINA from amino acid 6–364 (Figure 1). The *N. crassa*

TINA-like protein (NCU04570.1) is predicted to be significantly larger (119 kDa) than TINA (62 kDa) because of a large C-terminal extension. On BLAST analysis, this extension shows no similarities in the databanks at National Center for Biotechnology Information nor in the available *A. fumigatus* sequence. However, there is a highly TINA-related protein encoded in the genome of *A. fumigatus* (BLAST score 1193 and E value 9.0e-160. Preliminary sequence data was obtained from The Institute for Genomic Research Web site at http://www.tigr.org.).

TINA Interacts with NIMA in a Cell Cycle-specific Manner

To investigate the potential physical interaction between NIMA and TINA, strains were developed containing an extracopy of HA-tagged TINA expressed from the *alcA* promoter (Waring *et al*., 1989) in a *nimT23*^{cdc25} background. Another haploid strain was developed containing *nimA* also expressed from the *alcA* promoter in the *nimT23*^{cdc25} background. Stable diploids were generated from these strains by using forcing nutritional markers. The diploid (D31) is homozygous for *nimT23*^{cdc25} and also contains a copy of HA-tagged TINA and a copy of *nimA* expressed from the *alcA* promoter. By temperature shifts, we could generate a synchronous G_2 arrest and release into mitosis. A rich media was developed (see MATERIALS AND METHODS) such that low expression from the *alcA* promoter could be achieved. Under these conditions, less than double the endogenous amount of TINA was expressed and the expression level of NIMA was similarly low, causing no effects on mitotic progression (our unpublished data).

Immunoprecipitation experiments using proteins derived from cell cycle-staged cultures indicate that TINA and NIMA physically interact and show that this interaction is regulated. At the G_2 arrest point of *nimT23*^{cdc25}, when TINA is immunoprecipitated NIMA can be readily detected in the precipitates (Figure 2A). However, within 5 min of entry into mitosis this interaction is dramatically reduced, suggesting a G_2-specific interaction between TINA and NIMA. A similar pattern of interaction was revealed if NIMA was immunoprecipitated and TINA detected, but in this instance some residual interaction could also be detected in the samples progressing through mitosis. This experiment was repeated three times with almost identical results, although the amount of TINA detected in the NIMA precipitates in the samples released into mitosis was highest for this particular experiment (Figure 2A).

It is also clear from these experiments that the TINA protein becomes modified during mitosis such that its mobility is reduced during SDS-PAGE separation. This can be seen when TINA is immunoprecipitated and blotted (Figure 2A). Although no clear banding could be detected, there is a larger version(s) of TINA generated after activation of *nimT*^{cdc25} and entry into mitosis. However, in the NIMA immunoprecipitates, at least two bands of TINA with lower mobility can be resolved in the samples released from the G_2 arrest into mitosis (Figure 2A). These TINA mobility changes are reminiscent of the mobility shifts reported previously for NIMA during mitosis, which is caused by mitotic-specific phosphorylation (Ye *et al*., 1995)

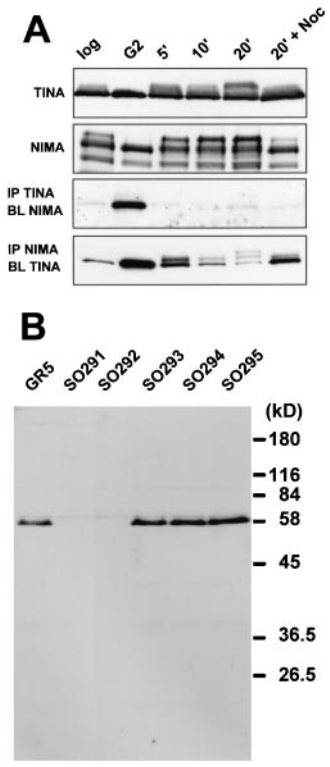

Figure 2. (A) NIMA and TINA interaction is cell cycle regulated. Protein was extracted from diploid strain D31 grown to mid-log phase (log) and then shifted to 42°C for 3 h to arrest cells in G_2 (G2) before releasing into mitosis. Samples were taken at 5, 10, and 20 min (5′, 10′, 20′) or after 20 min in the presence of nocodazole to cause a pseudomitotic arrest (20′ + Noc). The protein immunoprecipitated (IP) and detected (BL) is indicated to the left. (B) Lack of TINA protein in *tinA* deleted strains. Protein extracts were prepared from a wild-type strain (GR5), two strains with deletion of *tinA* as determined by PCR and Southern blotting (SO291 and SO292) and three strains without the deletion (SO293, SO294, SO295). Western blotting was completed using the TINA-specific affinity-purified anti-peptide antibody DELGEL. Equal loading and transfer of protein in each lane was confirmed by Ponceau Red staining of the nitrocellulose filter. Mobility of marker proteins is indicated to the right.

TINA Locates to the Spindle Pole Bodies during Mitosis

We undertook to see whether TINA is located within the cell in a manner indicative of a role in cell cycle progression. Initially, we used a haploid strain containing the *nimT23*^{cdc25} mutation and a HA-tagged version of TINA expressed from the *alcA* promoter. The cells were grown in media allowing mild expression of *alcA*::HA-tagged TINA and were then blocked in G_2 and released into mitosis by using temperature shifts. At the G_2 arrest point of *nimT23*^{cdc25} no specific localization was observed for HA-TINA (Figure 3, A and B), but upon release into mitosis, two dots of HA-TINA staining became apparent that were always in the vicinity of nuclei (Figure 3, C and D). By observing the degree of condensation and separation of nuclear DNA, it was clear that HA-TINA localized to two foci associated with nuclei throughout mi-

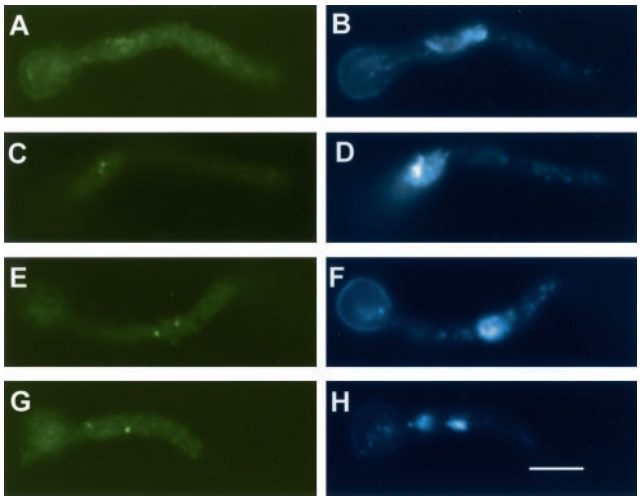

Figure 3. TINA locates to nuclear dots at mitosis. Cells containing the *nimT23* mutation, which expressed HA-tagged TINA, were arrested in G_2 (A and B) and released into mitosis (C–H) by temperature shift and cells processed to visualize TINA by using anti-HA antibodies (A, C, E, and G) and DAPI to reveal DNA. Samples at various stages of mitosis are shown demonstrating lack of TINA staining at the G_2 SPBs but positive location during mitotic progression. Bar, ~5 μM.

tosis (Figure 3, C–H). However, no clear pattern of staining was apparent either before or after mitosis. An identical pattern was observed in randomly growing cells although in this case a low percentage of cells displayed some nuclear staining as well (our unpublished data).

As the foci of TINA strongly suggested localization at the SPBs during mitosis, cells were stained to reveal microtubules by using α-tubulin-specific antibodies along with TINA-specific antibodies. Mitotic spindles were seen to have TINA located at their ends (Figure 4) as expected of a protein located at the SPBs.

The dynamic localization of TINA to SPBs was quantitated during a synchronous mitosis generated by temperature shift of a *nimT23*^{cdc25} strain. At the G_2 arrest point of *nimT23*^{cdc25} no TINA could be observed at the spindle poles. On release into mitosis a synchronous wave of TINA localization to the SPBs was observed peaking at 10 min after release into mitosis and reducing as cells exited mitosis (Figure 4, graph). A matching increase of the spindle mitotic index was also observed to peak at the 10-min time point.

To determine whether localization of TINA to the SPB was dependent upon the function of microtubules, a release into mitosis was completed in the presence of the microtubule poison nocodazole. Such cells entered a mitotic state as revealed by an increase in the chromosome mitotic index (>80% from 10 min on). However, the localization of TINA to the SPB was dramatically reduced under these conditions (Figure 4, graph), indicating that functional microtubules are required for location of TINA to the SPB.

To see whether the localization of TINA to the SPB required mitotic activation of NIMA, cells containing the *nimA5* mutation (LPW75) were shifted to 42°C to arrest them in G_2 without *nimA* function. Cells were fixed and stained for TINA by using affinity-purified peptide-specific antibodies. The cells were also stained with DAPI to reveal DNA and with the γ-tubulin–specific antibody GTU-88 to locate SPBs (Oakley *et al.*, 1990). Each G_2 nucleus correlated with a single paired SPB but only 3% of these had any TINA specific staining (our unpublished data). In contrast, upon

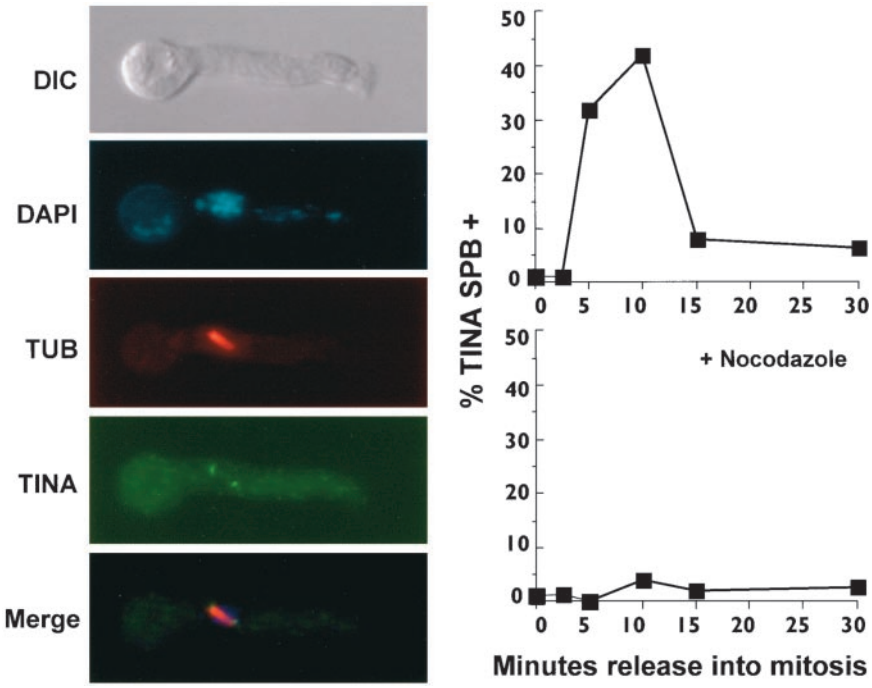

Figure 4. Micrograph shows that TINA localizes to the ends of spindles at mitosis. A metaphase cell is shown with, from the top, a differential interference contrast image, DAPI staining revealing condensed DNA, tubulin staining of the mitotic spindle, TINA staining, and a merge. The graph at right shows the kinetics of localization of TINA to spindle poles during synchronous mitosis. A strain containing the *nimT23* mutation that expressed HA-tagged TINA was arrested at G_2 by shift to 42°C for 3 h (time 0) before downshift to 30°C to allow entry into mitosis (as in Figure 3). The percentage of cells displaying SPB localization of TINA was determined using immunofluorescence. Another culture, as indicated, was treated with nocodazole before release into mitosis.

release to permissive temperature for *nimA5*, cells entered mitosis within 5 min and their nuclei had two closely located SPBs associated with condensed DNA. The SPBs of >88% of such mitotic nuclei were positive for TINA (our unpublished data). This indicates that TINA localization to the SPB is dependent upon activation of NIMA at G_2.

Because these experiments follow endogenous TINA, the data also demonstrate that the studies using HA-tagged TINA reflect the localization of TINA and are not an artifact of the HA tag or expression from the *alcA* promoter. The colocalization of endogenous TINA with γ-tubulin (Oakley *et al*., 1990) also confirms the SPB localization of this protein at mitosis (our unpublished data).

Because the localization of TINA is dynamic, we wished to view its changes through the cell cycle in living cells. To do this, *tinA* was tagged with plant-adapted GFP (Fernandez-Abalos *et al*., 1998) under control of the *alcA* promoter. Transformants were identified that expressed no more than the endogenous level of TINA, and live cell imaging studies were completed. Cells were examined during normal progression through the cell cycle and after block release experiments by using TINA-GFP expressed in *nimA5* or *nimT23* containing strains to generate synchronous entry into and through mitosis. The results confirmed our conclusions from study of fixed cells that TINA locates to the SPBs specifically at mitosis (our unpublished data). The data also indicate the dynamic localization revealed for TINA by using immunofluorescence is not caused by the potential masking/unmasking of antibody epitopes.

Deletion of tinA

A construct that replaced the entire *tinA* coding sequence with a deletion cassette containing *pyrG* was generated using homologous recombination into a *tinA* containing BAC with *E. coli* strain DY380 (Lee *et al*., 2001). Southern blot and PCR analysis of 20 transformants identified two strains with clean *tinA* deletions (our unpublished data). These two *tinA*-deleted strains, and three control transformants, were analyzed by Western blotting with TINA-specific antibodies. The results confirmed that *tinA* was deleted from these two strains demonstrating *tinA* to be a nonessential gene (Figure 2B).

The *tinA* deleted strains were tested for sensitivity/resistance to the DNA-damaging agent MMS, the DNA synthesis inhibitor hydroxyurea, the microtubule poison nocodazole, high osmolarity, and growth at 20°C, 37°C, and 42°C. Under all tested conditions, they grew and developed normally compared with control strains. Neither conidia (asexual spores) nor germlings from the *tinA*-deleted strains were sensitive to UV irradiation, and both deleted strains underwent self crosses and crosses to other strains to yield normal meiotic progeny.

A Role for tinA during Mitosis

To further investigate the potential role of TINA in cell cycle progression, Δ*tinA* double mutants were generated with a range of cell cycle mutations (*sonA1*, *nimA1*, *nimA5*, *nimA7*, *bimE7*, *nimE6*, *nimT23*, *nimX1*, *nimX2*, and *nimX3*) and tested for synthetic lethality. Only the *bimE7*/Δ*tinA* double mutant displayed increased temperature sensitivity compared with the two single mutants (Figure 5). The *bimE7* mutation is in

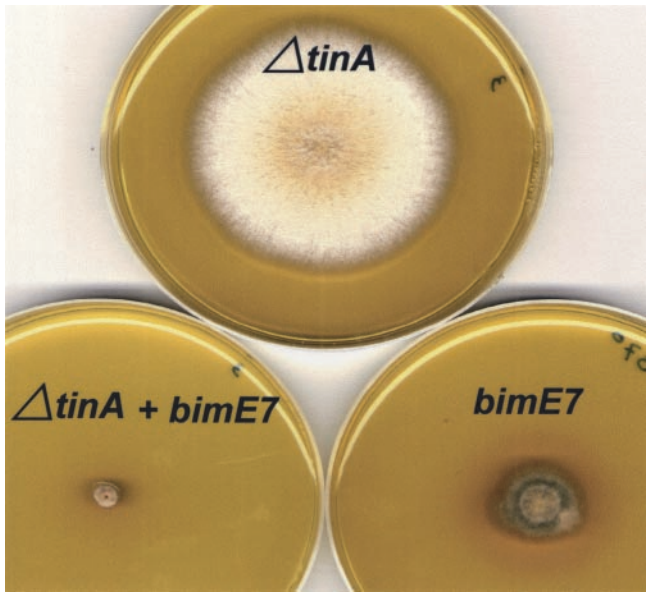

Figure 5. Synthetic lethality between Δ*tinA* and *bimE7*. Strains with the indicated pertinent genotypes were point inoculated and grown at 37°C for 3 d before photography. Strains were SO292 (Δ*tinA*) DBE4 (*bimE7*) and SO326 (Δ*tinA*/*bimE7*).

the APC1 component of the APC/C (Peters *et al*., 1996; Zachariae *et al*., 1996) and causes a prolonged arrest in metaphase at restrictive temperature (Morris, 1976; Osmani *et al*., 1988a).

The synthetic lethality between Δ*tinA* and *bimE7* indicated that metaphase arrest may be detrimental in the absence of TINA. However, lack of TINA did not significantly change the kinetics of the mitotic arrest caused by *bimE7*, with both *bimE7* and *bimE7*/Δ*tinA* strains reaching a peak spindle mitotic index of 80–96% at 2.5–3.0 h (normal spindle mitotic index is ~4%). The *bimE7* mutation caused an arrest at metaphase (Osmani *et al*., 1988a) with short spindles and DNA located centrally on the spindle (Figure 6, A1-A4), typical of mutations in subunits of the APC/C. Few astral microtubules were observed with <17% of spindles at the *bimE7* arrest having any microtubules emanating from the SPBs into the cytoplasm.

Initial observations of the double *bimE7*/Δ*tinA* strain suggested that lack of *tinA* perhaps allowed progression past metaphase into anaphase because some spindle-like structures were seen with separated DNA apparently at their poles (Figure 6, B1–B3). This seemed an unlikely outcome and, because the cells in question were of a size typical of cells with four nuclei and the "spindles" in question looked unusual, we considered alternative explanations.

Interestingly, >70% of the spindles in the *bimE7*/Δ*tinA* cells had marked astral microtubule bundles emanating from their SPBs into the cytoplasm. This can be seen in Figure 6, C1–C3, where the spindle in the right of the cell has a clear bundle of astral microtubules projecting toward the tip of the cell as indicated. We considered that these astral bundles could potentially interact in the cytoplasm, giving the appearance of a telophase spindle as noticed in Figure 6B. Indeed, we were able to observe many examples, in

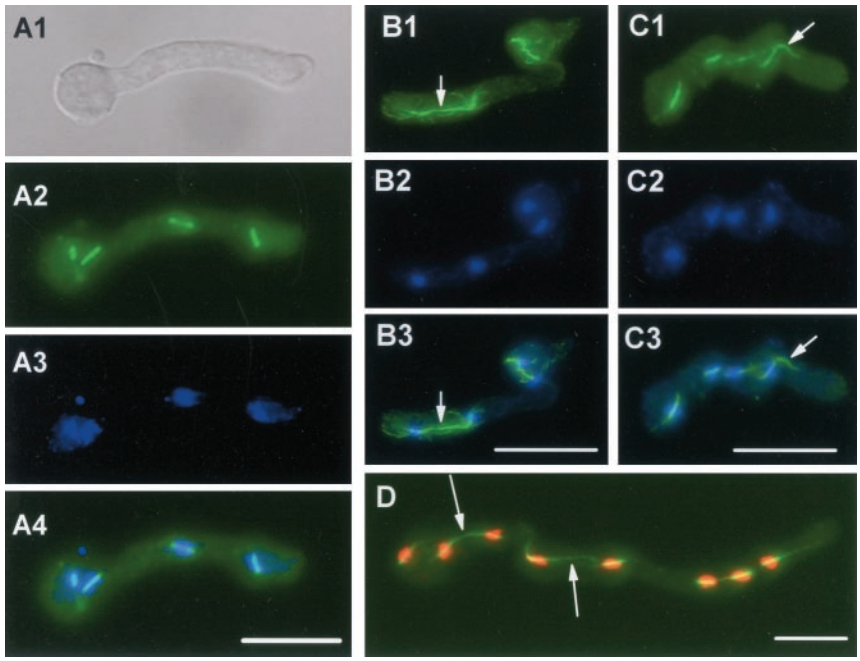

Figure 6. (A1–A4) Typical metaphase-arrested spindle lacking astral microtubules after inactivation of *bimE*. A *bimE7* strain (DBE4) was germinated at permissive temperature for a period to allow germination before shift to restrictive temperature of 42°C for 2 h. Cells were fixed and processed for immunofluorescence to visualize microtubules (A2) and stained with DAPI to reveal DNA (A3). A differential interference contrast image (A1) and a merge of the microtubule and DNA image (A4) are also shown. (B1–B3 and C1–C3 and D). Astral microtubules in a *bimE7* + Δ*tinA* double mutant. A *bimE7*/Δ*tinA* strain (SO326) was geminated at permissive temperature for a period to allow germination before shift to restrictive temperature (42°C) for 2 h. Cells were fixed and processed to visualize microtubules (green) and stained with DAPI to reveal DNA (blue, but red in D to better distinguish individual nuclei in this cell). Arrows in B indicate a spindle-like structure stretching between DNA. Arrow in C indicates a bundle of astral microtubules. Arrows in D indicate astral microtubule bundles beginning to interact between nuclei. Bar, ~5 μM.

multiple experiments, of astral microtubules interacting as shown in Figure 6D. In this cell, the arrows indicate astral microtubules just beginning to interact between different nuclei. We therefore conclude that, rather than allowing progression of anaphase in the absence of BIME function, lack of TINA allows enhanced astral microtubule formation. These microtubule bundles then seem to interact, giving the appearance of abnormal telophase-like spindle formation (Figure 6B).

To confirm that lack of *tinA* causes changes in the microtubule organizing capacity of the SPB during metaphase arrest, allowing spindles to interact via their astral microtubules, we generated strains expressing GFP-tagged *tubA* (Han *et al*., 2001) to visualize microtubules in real time. We first observed astral microtubule architecture during a normal mitosis. Consistent with previous observations of fixed cells, astral microtubules are largely absent from spindles during metaphase but become more apparent during anaphase B, as the metaphase spindle begins to elongate (see supplemental movies A [video-A.mov] and B [video-B.mov]). As the metaphase spindle begins to elongate during anaphase B, astral microtubules develop in the cytoplasm in all directions from the SPB. These microtubules then repopulate the cytoplasm with interphase microtubule arrays during G1.

Similar microscopy was used to determine the microtubule architecture during a metaphase arrest by using the temperature-sensitive *bimE7* mutation to inactivate the APC/C. Using a heated culture dish, and a heated objective, a strain with *bimE7* and GFP-tagged tubulin was heated to 42°C with recordings beginning 2 h after the shift to allow cells time to begin to arrest at metaphase. Figure 7A shows five *bimE7* cells at 15 min (910 s) during a recording >40 min [video-C.mov]. At this time point, 14 spindles can be seen and very few, if any, astral microtubules can be distinguished. During 10 such recordings, we have been able to see some short lived astral microtubules that all undergo catastrophe within minutes of being formed.

To determine the effect of lack of *tinA*, live imaging of microtubules in a *bimE7*/Δ*tinA* + GFP-*tubA* strain was performed exactly as described for the *bimE7* cells with very different results. Lack of *tinA* did not change the timing of the metaphase arrest but did markedly change the microtubule architecture compared with the *bimE7* cells. Metaphase-arrested cells displayed many spindles with astral microtubules. In many instances, these astral microtubules interacted between different spindles, leading to the appearance of large spindle like-structures containing more than one spindle. The accompanying movie [video-D.mov] shows that lack of *tinA* during a *bimE7* imposed metaphase arrest leads to many astral microtubules being formed at metaphase and that these astral microtubules often interact. Most commonly, this leads to formation of tandem spindles connected in series by their astral microtubules (Figure 7B, two examples marked by arrowheads). In addition, spindles positioned side by side often have their astral microtubules interact forming square like structures (see last frame of video-D.mov, cell marked with *). Neither of these phenomena was seen during comparable *bimE7* arrests. This live imaging analysis further demonstrates that lack of *tinA* at the SPB leads to formation of very atypical metaphase arrested spindles that can interact via their astral microtubules in a manner not seen during normal metaphase arrest.

DISCUSSION

Proteins able to interact with *A. nidulans* NIMA in the yeast two-hybrid system have provided insights into how mitosis is regulated from fungi to humans (Lu *et al*., 1996; Crenshaw *et al*., 1998; Shen *et al*., 1998; Lu *et al*., 2002). With this in mind, we have isolated new NIMA-interactive proteins by

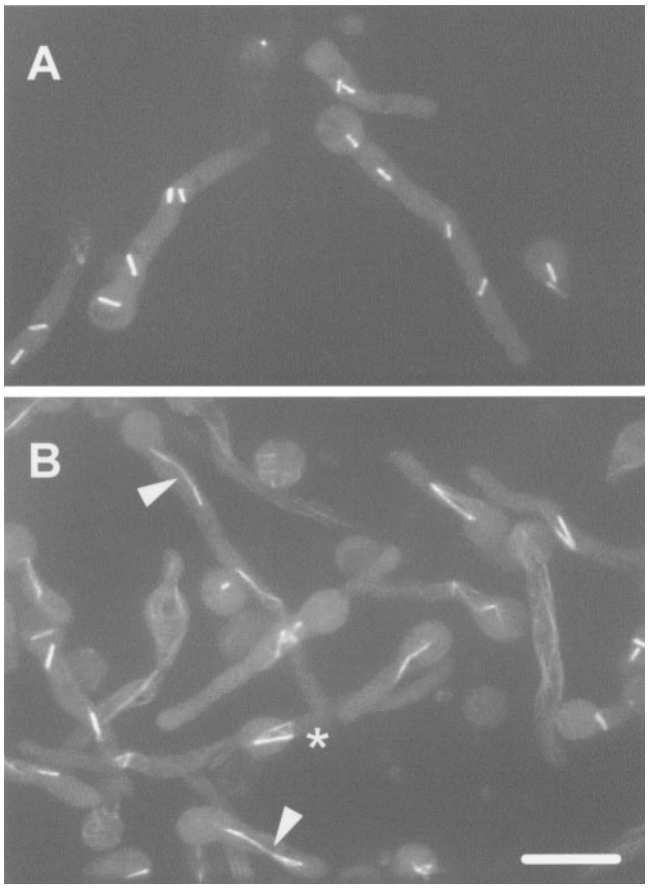

Figure 7. Live cell microtubule architecture during a *bimE7* imposed metaphase arrest with *tinA* (A) and without *tinA* function (B). Cells containing *bimE7* + GFP-*tubA* (A) or *bimE7*/Δ*tinA* + GFP-*tubA* (B) were shifted to 42°C to impose metaphase arrest by inactivation of *bimE7*. Cells were viewed using a spinning disk confocal microscope and the micrographs are maximum intensity projections of a Z-series stack taken from video-C.mov (A) and video-D.mov (B) from the 15-min exposure (910 s) during recordings >40 min. Arrowheads in B indicate spindle joined by astral microtubules. The * indicates parallel spindles with their astral microtubules interacting which form a square like structure by the end of the video. Bar, ~5 μM.

using the two-hybrid approach and tested them for cell cycle effects when overexpressed. This approach identified two new NIMA-interactive proteins causing arrest in interphase (Davies and Osmani, unpublished data). However, the TINA protein, although able to interact strongly with NIMA, had no apparent effects when overexpressed (our unpublished data), but further study of TINA has indicated that it may play a role in microtubule formation at mitosis.

TINA contains potential coiled-coil domains, as does NIMA and some other NIMA interactive proteins, suggesting this motif may play a role in their binding together. Data from immunoprecipitation experiments indicate that TINA and NIMA bind to each other, and that this binding is regulated during the cell cycle. From repeated experiments, TINA and NIMA bind most strongly during G_2 arrest. At this point in the cell cycle neither NIMA (De Souza *et al*., 2000) or TINA have a defined localization. On mitotic initiation, the interaction between TINA and NIMA is diminished and they localize to different parts of the cell. TINA rapidly concentrates to the separating SPBs as the bipolar spindle is beginning to form. However, although NIMA localizes to the SPBs at mitosis, it first localizes to the nuclear DNA and to the SPBs after metaphase (De Souza *et al*., 2000). Early in mitosis, TINA and NIMA therefore localize to different parts of the mitotic machinery, with TINA concentrated at the spindle poles, whereas NIMA is associated with nuclear DNA. Later during mitosis, both TINA and NIMA are localized to the spindle poles, leaving open the potential that TINA may act as a landing site for NIMA at the spindle poles at anaphase.

Whether TINA and NIMA interact during mitosis remains somewhat of an open question. For instance, if we first immunoprecipitate TINA and probe for NIMA there is apparently little or no interaction between these two proteins during mitosis. On the other hand, if we first immunoprecipitate NIMA then probe for TINA there is still some interaction that, although somewhat variable between experiments, was detectable in all experiments completed. Control immunoprecipitates failed to reveal nonspecific precipitation of TINA. The two sets of immunoprecipitation experiments therefore yield contradictory data regarding the degree of NIMA-TINA binding during mitosis. One explanation could be that the immunoprecipitation of TINA does not bring down the mitotic complex due to antigen exclusion in this complex, or the binding of the TINA-precipitating antibody could perhaps change the conformation of TINA to reduce binding of NIMA in the mitotic complex. Whatever the reason for the lack of NIMA in TINA immunoprecipitates from mitotic extracts, these two proteins do locate transiently to the SPB during the latter part of mitosis.

Because of the cell cycle-specific modification of TINA, its regulated interaction with NIMA, and its mitotic specific localization to the SPBs during mitosis, we had anticipated that deletion of *tinA* would cause mitotic defects, perhaps leading to lethality. However, deletion of *tinA* failed to reveal a clear phenotype, although synthetic lethality was observed with *bimE7* (see below). Lack of effect during normal growth may be due to redundancy with another gene having overlapping functions. However, only a single TINA-like protein could be detected in the genomes of *A. fumigatus* or *N. crassa*, suggesting that in filamentous fungi only one TINA-like protein is present.

Another explanation for lack of lethality after deletion of TINA would be if its function were not essential. Although NIMA is essential for mitotic progression in *A. nidulans* (Ye *et al*., 1998) the NIMA-l*ike* Fin1p kinase of *S. pombe* is nonessential (Grallert and Hagan, 2002; Krien *et al*., 1998) but does play a role in mitotic regulation (Krien *et al*., 2002). Fin1p has therefore been proposed to play a fine-tuning role for mitotic progression and TINA could also be involved in such fine-tuning nonessential mitotic functions.

One such mitotic function is suggested from studies of *bimE7*/Δ*tinA* double mutant strains. Lack of TINA causes synthetic lethality when APC/C function is partially compromised. The most marked phenotype observed in this double mutant was a striking increase in bundles of microtubules emanating away from the spindle, which then inter-

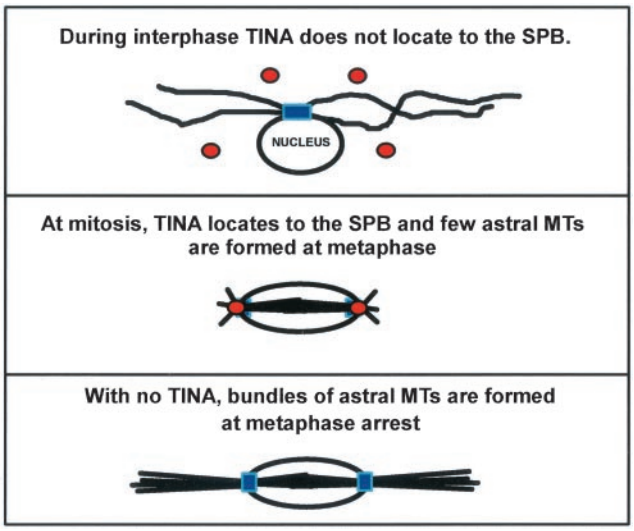

Figure 8. Perhaps TINA is involved in modifying the SPB at mitosis to control the number of astral microtubules organized at metaphase. Spindle pole bodies are depicted in blue and TINA in red. During interphase the SPB nucleates cytoplasmic microtubules, TINA is not located to the SPBs, and no mitotic spindle is present. During metaphase, spindle formation is apparent, TINA is located to the SPBs, and few astral microtubules are formed (see video-C.mov). Without TINA function, bundles of astral microtubules are formed from the SPBs during metaphase arrest that are normally suppressed by TINA located at the SPBs. These microtubule bundles sometimes then interact as shown in the video-D.mov.

acted to join spindles together in series. These phenomena were first implied from fixed cell samples and subsequently confirmed using live cell imaging of microtubule architecture.

At the time when TINA locates to the SPB during initiation of mitosis there is a major restructuring of the microtubule cytoarchitecture. Cytoplasmic microtubules are disassembled and the mitotic spindle forms within nuclei. The SPB therefore nucleates cytoplasmic microtubules during interphase but switches to nucleate microtubules in the nucleus to orchestrate spindle formation during mitosis. After completion of mitosis, and return to interphase, this is reversed, with the SPB again organizing cytoplasmic microtubules as the nuclear spindle microtubules disappear. Little is currently known about how the nucleating capacity of the SPB undergoes such dramatic changes during transition from interphase to mitosis and back to interphase. Because of the localization of TINA to the SPB during mitosis, and the effects of lack of TINA during metaphase arrest, we speculate that TINA is involved in regulation of the cytoplasmic microtubule organizing capacity of the SPB during mitosis. The potential role for TINA in helping regulate microtubule formation during mitosis is shown in Figure 8. Although this role may not be essential, it could become more important during an extended arrest at metaphase during which excessive microtubule nucleation can occur.

Because NIMA localizes to the spindle and SPB during mitosis, and is required for spindle formation, it likely plays a role in spindle formation. It is of note that induction of full-length NIMA is able to affect microtubule architecture, promoting formation of transient spindle-like structures (Osmani *et al*., 1988b). Additionally, forcing cells into mitosis without normal NIMA activity by mutation of the *bimE* APC/C component causes marked mitotic defects with SPBs unable to nucleate normal bipolar spindles in the absence of fully active NIMA (Osmani *et al*., 1991b). Data from other systems also support a role for NIMA-related kinases in spindle formation (Grallert and Hagan, 2002; Krien *et al*., 2002). The current work indicates a potential role for the NIMA interacting protein TINA in astral microtubule formation during mitosis. Further analysis of TINA may provide an understanding of how the microtubule nucleating capacity of the SPB is so dramatically modified during the G_2-M-G_1 transitions.

ACKNOWLEDGMENTS

We thank our colleagues in the laboratory for help and suggestions, particularly Dr. Colin De Souza. Thanks are also extended to Drs. Chrisophe d'Enfert and Don Court for plasmids and guidance with recombination constructs. This work was supported by grants from the National Institutes of Health (GM 42564 to S.A.O. and GM 31837 to B.R.O.).

REFERENCES

Bussink, H.J., and Osmani, S.A. (1998). A cyclin-dependent kinase family member (PHOA) is required to link developmental fate to environmental conditions in *Aspergillus nidulans.* EMBO J. *17*, 3990–4003.

Chaveroche, M. K., Ghigo, J. M., and d'Enfert, C. (2000). A rapid method for efficient gene replacement in the filamentous fungus *Aspergillus nidulans.* Nucleic Acids Res. *28*, E97.

Chen, A., Yanai, A., Arama, E., Kilfin, G., and Motro, B. (1999). NIMA-related kinases: isolation and characterization of murine nek3 and nek4 cDNAs, and chromosomal localization of nek1, nek2 and nek3. Gene *234*, 127–137.

Crenshaw, D.G., Yang, J., Means, A.R., and Kornbluth, S. (1998). The mitotic peptidyl-prolyl isomerase, Pin1, interacts with Cdc25 and Plx1. EMBO J. *17*, 1315–1327.

De Souza, C.P., Osmani, A.H., Wu, L.P., Spotts, J.L., and Osmani, S.A. (2000). Mitotic histone H3 phosphorylation by the NIMA kinase in *Aspergillus nidulans.* Cell *102*, 293–302.

Doonan, J.H., MacKintosh, C., Osmani, S., Cohen, P., Bai, G., Lee, E.Y.C., and Morris, N.R. (1991). A cDNA encoding rabbit muscle protein phosphatase 1α complements the *Aspergillus* cell cycle mutation, bimG11. J. Biol. Chem. *266*, 18889–18894.

Doshi, P., Bossie, C.A., Doonan, J.H., May, G.S., and Morris, N.R. (1991). The two alpha-tubulin genes of *Aspergillus nidulans* encode divergent proteins. Mol. Gen. Genet. *225*, 129–141.

Dunne, P.W., and Oakley, B.R. (1988). Mitotic gene conversion, reciprocal recombination and gene replacement at the *benA*, beta-tubulin locus of *Aspergillus nidulans.* Mol. Gen. Genet. *213*, 339–345.

Fernandez-Abalos, J.M., Fox, H., Pitt, C., Wells, B., and Doonan, J.H. (1998). Plant-adapted green fluorescent protein is a versatile vital reporter for gene expression, protein localization and mitosis in the filamentous fungus, *Aspergillus nidulans.* Mol. Microbiol. *27*, 121–130.

Fry, A.M., Mayor, T., Meraldi, P., Stierhof, Y.D., Tanaka, K., and Nigg, E.A. (1998a). C-Nap1, a novel centrosomal coiled-coil protein and candidate substrate of the cell cycle-regulated protein kinase Nek2. J. Cell Biol. *141*, 1563–1574.

Fry, A.M., Meraldi, P., and Nigg, E.A. (1998b). A centrosomal function for the human Nek2 protein kinase, a member of the NIMA family of cell cycle regulators. EMBO J. *17*, 470–481.

Fry, A.M., Schultz, S.J., Bartek, J., and Nigg, E.A. (1995). Substrate specificity and cell cycle regulation of the Nek2 protein kinase, a potential human homolog of the mitotic regulator NIMA of *Aspergillus nidulans.* J. Biol. Chem. *270*, 12899–12905.

Grallert, A., and Hagan, I.M. (2002). Schizosaccharomyces pombe NIMA-related kinase, Fin1, regulates spindle formation and an affinity of Polo for the SPB. EMBO J. *21*, 3096–3107.

Ha, K.Y., Yeol, C.J., Jeong, Y., Wolgemuth, D.J., and Rhee, K. (2002). Nek2 localizes to multiple sites in mitotic cells, suggesting its involvement in multiple cellular functions during the cell cycle. Biochem. Biophys. Res. Commun. *290*, 730–736.

Han, H., Liu, B., Zhang, J., Zuo, W., and Morris, N.R. (2001). The *Aspergillus* cytoplasmic dynein heavy chain and NUDF localize to microtubule ends and affect microtubule dynamics. Curr. Biol. *11*, 719–724.

Helps, N.R., Luo, X., Barker, H.M., and Cohen, P.T. (2000). NIMA-related kinase 2 (Nek2), a cell-cycle-regulated protein kinase localized to centrosomes, is complexed to protein phosphatase 1. Biochem. J. *349*, 509–518.

Holland, P.M., Milne, A., Garka, K., Johnson, R.S., Willis, C.R., Sims, J.E., Rauch, C.T., Bird, T.A., and Virca, G.D. (2002). Purification, cloning and characterization of Nek8, a novel NIMA-related kinase, and its candidate substrate Bicd2. J. Biol. Chem. *277*, 16229–16240.

Kandli, M., Feige, E., Chen, A., Kilfin, G., and Motro, B. (2000). Isolation and characterization of two evolutionarily conserved murine kinases (Nek6 and nek7) related to the fungal mitotic regulator, NIMA. Genomics *68*, 187–196.

Krien, M.J., Bugg, S.J., Palatsides, M., Asouline, G., Morimyo, M., and O'Connell, M.J. (1998). A NIMA homologue promotes chromatin condensation in fission yeast. J. Cell Sci. *111*, 967–976.

Krien, M.J., West, R.R., John, U.P., Koniaras, K., McIntosh, J.R., and O'Connell, M.J. (2002). The fission yeast NIMA kinase Fin1p is required for spindle function and nuclear envelope integrity. EMBO J. *21*, 1713–1722.

Lee, E.C., Yu, D., Martinez, dV, Tessarollo, L., Swing, D.A., Court, D.L., Jenkins, N.A., and Copeland, N.G. (2001). A highly efficient *Escherichia coli*-based chromosome engineering system adapted for recombinogenic targeting and subcloning of BAC DNA. Genomics *73*, 56–65.

Letwin, K., Mizzen, L., Motro, B., Ben-David, Y., Bernstein, A., and Pawson, T. (1992). A mammalian dual specificity protein kinase, Nek1, is related to the NIMA cell cycle regulator and highly expressed in meiotic germ cells. EMBO J. *11*, 3521–3531.

Lu, K.P., Hanes, S.D., and Hunter, T. (1996). A human peptidyl-prolyl isomerase essential for regulation of mitosis. Nature *380*, 544–547.

Lu, K.P., and Hunter, T. (1995a). Evidence for a NIMA-like mitotic pathway in vertebrate cells. Cell *81*, 413–424.

Lu, K.P., and Hunter, T. (1995b). The NIMA kinase: A mitotic regulator in *Aspergillus nidulans* and vertebrate cells. Prog. Cell Cycle Res. *1*, 187–205.

Lu, K.P., Liou, Y.C., and Zhou, X.Z. (2002). Pinning down proline-directed phosphorylation signaling. Trends Cell Biol. *12*, 164–172.

Morris, N.R. (1976). A temperature-sensitive mutant of *Aspergillus nidulans* reversible blocked in nuclear division. Exp. Cell Res. *98*, 204–210.

Oakley, B.R., Oakley, C.E., and Rinehart J.E. (1987). Conditionally lethal *tubA* alpha-tubulin mutations in *Aspergillus nidulans.* Mol. Gen. Genet. *208*, 135–144.

Oakley, B.R., Oakley, C.E., Yoon, Y., and Jung, M.K. (1990). Gamma-tubulin is a component of the spindle pole body that is essential for microtubule function in *Aspergillus nidulans.* Cell *61*, 1289–1301.

Oakley, B.R., and Osmani, S.A. (1993). Cell-cycle analysis using the filamentous fungus *Aspergillus nidulans.* In: The Cell Cycle, A Practical Approach, ed. P. Fantes and R. Brooks, 127–142. London: Academic Press.

O'Connell, M.J., Norbury, C., and Nurse, P. (1994). Premature chromatin condensation upon accumulation of NIMA. EMBO J. *13*, 4926–4937.

O'Farrell, P.H. (2001). Triggering the all-or-nothing switch into mitosis. Trends Cell Biol. *11*, 512–519.

Osmani, A.H., McGuire, S.L., and Osmani, S.A. (1991a). Parallel activation of the NIMA and p34cdc2 cell cycle-regulated protein kinases is required to initiate mitosis in *A. nidulans.* Cell *67*, 283–291.

Osmani, A.H., O'Donnell, K., Pu, R.T., and Osmani, S.A. (1991b). Activation of the *nimA* protein kinase plays a unique role during mitosis that cannot be bypassed by absence of the *bimE* checkpoint. EMBO J. *10*, 2669–2679.

Osmani, S.A., Engle, D.B., Doonan, J.H., and Morris, N.R. (1988a). Spindle formation and chromatin condensation in cells blocked at interphase by mutation of a negative cell cycle control gene. Cell *52*, 241–251.

Osmani, S.A., May, G.S., and Morris, N.R. (1987). Regulation of the mRNA levels of nimA, a gene required for the G2-M transition in *Aspergillus nidulans.* J. Cell Biol. *104*, 1495–1504.

Osmani, S.A., Pu, R.T., and Morris, N.R. (1988b). Mitotic induction and maintenance by overexpression of a G2-specific gene that encodes a potential protein kinase. Cell *53*, 237–244.

Osmani, S.A., and Ye, X.S. (1996). Cell Cycle regulation in *Aspergillus* by two protein kinases. Biochem. J. *317*, 633–641.

Peters, J., King, R.W., Hoog, C., and Kirschner, M.W. (1996). Identification of BIME as a subunit of the anaphase-promoting complex. Science *274*, 1199–1201.

Pontecorvo, G. (1953). The genetics of *Aspergillus nidulans.* In: Advances in Genetics, ed. M. Demerec, New York: Academic Press, 141–238.

Pu, R.T., Gang Xu, Wu, L., Vierula, J., O'Donnell, K., Ye, X., and Osmani, S.A. (1995). Isolation of a functional homolog of the cell cycle specific NIMA protein kinase and functional analysis of conserved residues. J. Biol. Chem. *271*, 18110–18116.

Pu, R.T., and Osmani, S.A. (1995). Mitotic destruction of the cell cycle regulated NIMA protein kinase of *Aspergillus nidulans* is required for mitotic exit. EMBO J. *14*, 995–1003.

Rhee, K., and Wolgemuth, D.J. (1997). The NIMA-related kinase 2, Nek2, is expressed in specific stages of the meiotic cell cycle and associates with meiotic chromosomes. Development *124*, 2167–2177.

Roig, J., Mikhailov, A., Belham, C., and Avruch, J. (2002). Nercc1, a mammalian NIMA-family kinase, binds the Ran GTPase and regulates mitotic progression. Genes Dev. *16*, 1640–1658.

Sambroook, J., Fritsch, E.F., and Maniatis, T. (1989). Molecular Cloning: A Laboratory Manual, Cold Spring Harbor, NY: Cold Spring Harbor Laboratory Press.

Schultz, S.J., Fry, A.M., Sutterlin, C., Ried, T., and Nigg, E.A. (1994). Cell cycle-dependent expression of Nek2, a novel human protein kinase related to the NIMA mitotic regulator of *Aspergillus nidulans.* Cell Growth Diff. *5*, 1–11.

Schultz, S.J., and Nigg, E.A. (1993). Identification of 21 novel human protein kinases, including 3 members of a family related to the cell cycle regulator *nimA* of *Aspergillus nidulans.* Cell Growth Diff. *4*, 821–830.

Shen, M., Stukenberg, P.T., Kirschner, M.W., and Lu, K.P. (1998). The essential mitotic peptidyl-prolyl isomerase Pin1 binds and regulates mitosis-specific phosphoproteins. Genes Dev. *12*, 706–720.

Swaminathan, S., Ellis, H.M., Waters, L.S., Yu, D., Lee, E.C., Court, D.L., and Sharan, S.K. (2001). Rapid engineering of bacterial artificial chromosomes using oligonucleotides. Genesis *29*, 14–21.

Tanaka, K., and Nigg, E.A. (1999). Cloning and characterization of the murine Nek3 protein kinase, a novel member of the NIMA family of putative cell cycle regulators. J. Biol. Chem. *274*, 13491–13497.

Uto, K., and Sagata, N. (2000). Nek2B a novel maternal form of Nek2 kinase, is essential for the assembly or maintenance of centrosomes in early *Xenopus* embryos. EMBO J. *19*, 1816–1826.

Waring, R.B., May, G.S., and Morris, N.R. (1989). Characterization of an inducible expression system in *Aspergillus nidulans* using alcA and tubulin-coding genes. Gene *79*, 119–130.

Wu, L., Osmani, S.A., and Mirabito, P.M. (1998). A role for NIMA in the nuclear localization of cyclin B in *Aspergillus nidulans.* J. Cell Biol. *141*, 1575–1587.

Ye, X.S., Fincher, R.R., Tang, A., O'Donnell, K., and Osmani, S.A. (1996). Two S-phase checkpoint systems, one involving the function of both BIME and Tyr15 phosphorylation of $p34^{cdc2}$, inhibit NIMA and prevent premature mitosis. EMBO J. *15*, 3599–3610.

Ye, X.S., Fincher, R.R., Tang, A., Osmani, A.H., and Osmani, S.A. (1998). Regulation of the anaphase-promoting complex/cyclosome by $BIMA^{APC3}$ and proteolysis of NIMA. Mol. Biol. Cell *9*, 3019–3030.

Ye, X.S., Xu, G., Pu, P.T., Fincher, R.R., McGuire, S.L., Osmani, A.H., and Osmani, S.A. (1995). The NIMA protein kinase is hyperphosphorylated and activated downstream of $p34^{cdc2}$/cyclin B: coordination of two mitosis promoting kinases. EMBO J. *14*, 986–994.

Yu, D., Ellis, H.M., Lee, E.C., Jenkins, N.A., Copeland, N.G., and Court, D.L. (2000). An efficient recombination system for chromosome engineering in *Escherichia coli.* Proc. Natl. Acad. Sci. USA *97*, 5978–5983.

Zachariae, W., Shin, T.H., Galova, M., Obermaier, B., and Nasmyth, K. (1996). Identification of subunits of the anaphase-promoting complex of *Saccharomyces cerevisiae.* Science *274*, 1201–1204.